

# Carbon Chain Length in a Novel Anticancer Aryl-Urea Fatty Acid Modulates Mitochondrial Targeting, Reactive Oxygen Species Production and Cell Killing

Yasmin A. Elmaghrabi,<sup>[a]</sup> Ariane Roseblade,<sup>[b]</sup> Khalilur Rahman,<sup>[a]</sup> Tristan Rawling,<sup>[b]</sup> and Michael Murray<sup>\*[a]</sup>

The cancer cell mitochondrion could be a promising target for the development of new anticancer agents. 16-([3-chloro-5-(trifluoromethyl)-phenyl]carbamoylamino)hexadecanoic acid (**2**) is a novel aryl-urea fatty acid that targets the mitochondrion in MDA-MB-231 breast cancer cells and activates cell death. In the present study, the relationships between alkyl chain length in **2** analogues, mitochondrial disruption and cell killing were evaluated. The chain-contracted C13-analogue **7c** optimally disrupted the mitochondrial membrane potential ( $IC_{50}$   $4.8 \pm 0.8 \mu M$ ). In addition, annexin V-FITC/7-AAD assays demonstrated

that **7c** was the most effective cell killing analogue and C11 BODIPY (581/591) assays demonstrated that **7c** was also most effective in generating reactive oxygen species in MDA-MB-231 cells. Together, carbon chain length is a key factor that determines the capacity of **2** analogues to disrupt the mitochondrial membrane, induce the production of reactive oxygen species and kill breast cancer cells. As an aryl-urea with enhanced activity and improved drug-like properties, **7c** may be a suitable lead molecule for entry into a program of development of these molecules as anticancer agents.

## Introduction

The mitochondrion has important roles in cell death and survival.<sup>[1]</sup> Functional differences between mitochondria in normal and cancer cells offer the opportunity to develop new classes of mitochondrion-targeted agents with selective anticancer activity.<sup>[2]</sup>

Dietary intake of  $\omega$ -3 polyunsaturated fatty acids ( $\omega$ -3 PUFAs) has been shown to decrease cancer progression by impairing protumorigenic processes.<sup>[3,4]</sup> Although the underlying mechanisms are unclear, it is now clear that  $\omega$ -3 PUFAs, such as eicosapentaenoic acid (EPA) and docosahexaenoic acid, undergo biotransformation to lipid mediators that decrease cancer cell viability.<sup>[5]</sup> In a previous study, we found that the cytochrome P450 (CYP)-derived  $\omega$ -3-17,18-epoxide of EPA attenuated endothelial cell viability by decreasing proliferation and promoting apoptosis, whereas the regioisomeric epoxides were inactive.<sup>[6]</sup> Consistent with these findings, synthetic  $\omega$ -3 epoxides of saturated fatty acids were also found to activate

apoptosis and necrosis in breast cancer cells.<sup>[7]</sup> However, the development of  $\omega$ -3 PUFA-derived epoxides as potential drugs is limited by the metabolic instability and rapid inactivation of the epoxide moiety *in vivo*. Indeed, coadministration of inhibitors of the enzyme soluble epoxide hydrolase, which converts fatty acid epoxides to the inactive dihydroxy analogues, was required for *in vivo* activity.<sup>[8,9]</sup>

To overcome these problems, bioisosteric replacement of the oxirane ring in fatty acid epoxides by a ureido moiety has been found to produce analogues that retain biological activity and have improved metabolic stability.<sup>[10,11]</sup> In the case of  $\omega$ -3-17,18-epoxy-EPA, the inclusion of an aromatic system substituted with strong electron-withdrawing groups at the meta- and para- positions produced aryl-ureas with *in vitro* and *in vivo* anticancer activity.<sup>[12,13]</sup> The prototypic agent CTU (16-([3-chloro-5-(trifluoromethyl)phenyl]carbamoylamino)hexadecanoic acid; **1** in Figure 1) activated anticancer cell death *in vitro* and *in vivo* by mitochondrial targeting, which disrupted the membrane potential that drives ATP production by oxidative phosphorylation.<sup>[12]</sup> However, the potency of **1** was relatively low and further structural modifications are required to optimise the activity of aryl-ureas and to develop an effective lead molecule. In subsequent structure-activity relationship studies directed towards optimisation of the aromatic substitution pattern, a structural isomer of **1**—16-([3-chloro-5-(trifluoromethyl)-phenyl]carbamoylamino)hexadecanoic acid (**2**; Figure 1) — was a more effective agent that could be used as a lead compound for further development.<sup>[13]</sup>

In the present study, a chain contraction strategy was used to identify the optimal alkyl chain length linking the urea and carboxylate groups in **2**. In addition to improving anticancer activity, chain contraction will also reduce compound lipophilicity and flexibility, thus providing more drug-like ana-

[a] Y. A. Elmaghrabi, K. Rahman, M. Murray  
Discipline of Pharmacology and Sydney Pharmacy School, Faculty of Medicine and Health, University of Sydney, Camperdown NSW 2006, Australia  
E-mail: michael.murray@sydney.edu.au

[b] A. Roseblade, T. Rawling  
School of Mathematical and Physical Sciences, Faculty of Science, University of Technology Sydney, Ultimo NSW 2007, Australia

Supporting information for this article is available on the WWW under <https://doi.org/10.1002/cmdc.202400281>

© 2024 The Authors. ChemMedChem published by Wiley-VCH GmbH. This is an open access article under the terms of the Creative Commons Attribution License, which permits use, distribution and reproduction in any medium, provided the original work is properly cited.

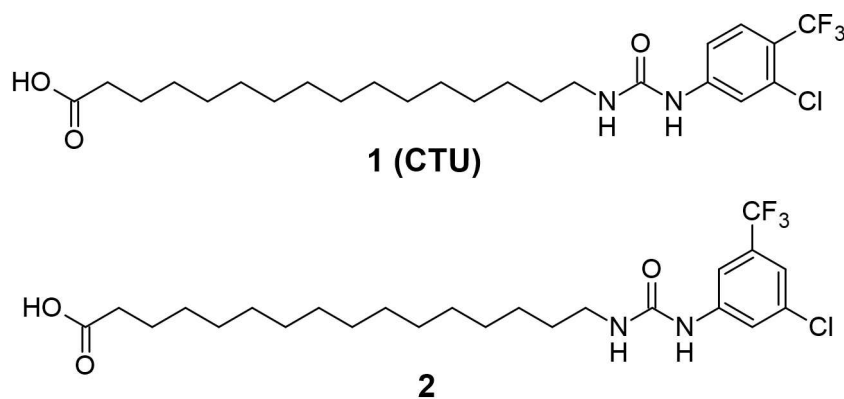


Figure 1. Chemical structures of the lead aryl-urea substituted fatty acids CTU (1) and 2.

logues for further optimisation. **2** contains a 16 carbon chain, and for this study a series of chain-contracted analogues (**7 a–e** that contained 11–15 methylene groups) was investigated. It was found that **2** analogues of intermediate carbon chain length, particularly **7 c**, which contained a 13 carbon chain, have superior antiproliferative and pro-apoptotic activities than **2**. **7 c** disrupted the mitochondrial membrane potential more effectively than **2** and has emerged as an aryl-urea with improved anticancer activity and hydrophobic properties and that could be more suited to drug development and formulation.

## Materials and Methods

### General Chemistry

The synthesis of **2** has been described previously.<sup>[13]</sup> Amines **3 a–c** and nitriles **4 a–b** were synthesised according to literature procedures.<sup>[13]</sup> All reagents were purchased from Fluorochem (Hadfield, Derbyshire, United Kingdom) and all anhydrous solvents were purchased from Sigma-Aldrich (Castle Hill, NSW, Australia). Reactions were monitored using thin-layer chromatography on Merck silica gel 60 F254 aluminium backed plates. Dry column vacuum chromatography was used to purify reaction products using Merck Kieselgel 60 (230–400 mesh) as the stationary phase. <sup>1</sup>H and <sup>13</sup>C NMR were recorded on an Agilent Technologies 500/40 NMR spectrometer. Spectra were referenced internally to residual solvents CDCl<sub>3</sub> (<sup>1</sup>H δ 7.26 ppm, <sup>13</sup>C δ 77.00 ppm) and DMSO-d<sub>6</sub> (<sup>1</sup>H δ 2.49 ppm, <sup>13</sup>C δ 39.52 ppm). <sup>1</sup>H NMR data are reported in order by chemical shift (δ in ppm), multiplicity (s=singlet, d=doublet, t=triplet, q=quartet, quin=quintet, dd=doublet of doublets, dt=doublet of triplets, ddd=doublet of doublet of doublets, td=triplet of doublets, m=multiplet, br=broad signal), the coupling constant (J in Hz) and signal integration. Melting points were determined using a Gallenkamp Melting Point Apparatus. High resolution mass spectrometry (HRMS) was performed on an Agilent Technologies 6510 Q-TOF LCMS.

### Synthesis

**N-[3-chloro-5-(trifluoromethyl)phenyl]imidazole-1-carboxamide (5)** 3-chloro-5-(trifluoromethyl)aniline (3.00 g, 15.3 mmol) and 1,1'-carbonyldiimidazole (2.49 g, 15.3 mmol) were dissolved in anhydrous dichloromethane (40 mL) and the reaction was stirred at room temperature for 2 h. The solvent was then removed under reduced pressure, yielding a crude product that was used without further purification.

### General Procedure for Synthesis of Ureas from Amines

To a solution of **3 a–c** (0.53 mmol) in dichloromethane (10 mL) was added **5** (0.230 g, ~0.80 mmol). The reaction mixture was stirred at room temperature for 1 h. Ethyl acetate (50 mL) was added and the solution was washed with water (3x50 mL). The organic layer was dried over sodium sulfate and evaporated under reduced pressure. The crude product was purified on silica gel using gradient elutions of dichloromethane/ethyl acetate (100:0–85:15).

**Ethyl 11-[[3-chloro-5-(trifluoromethyl)phenyl]carbamoylamino]undecanoate (6a).** White solid, 71 % yield. <sup>1</sup>H NMR (500 MHz, CDCl<sub>3</sub>): δ 7.66 (s, 1H), 7.60 (s, 1H), 7.45 (s, 1H), 7.19 (s, 1H), 5.38 (t, J=5.5 Hz, 1H), 4.14 (q, J=7.0 Hz, 2H), 3.22 (q, J=6.5 Hz, 2H), 2.31 (t, J=7.5 Hz, 2H), 1.61 (quin, J=7.5 Hz, 2H), 1.47 (quin, J=7.5 Hz, 2H), 1.35–1.20 (m, 15H). <sup>13</sup>C NMR (125 MHz, CDCl<sub>3</sub>): δ 174.68, 155.63, 141.18, 135.24, 132.43 (q, J=31 Hz), 123.15 (q, J=272 Hz), 121.82, 118.95 (q, J=6 Hz), 113.55 (q, J=6 Hz), 60.47, 40.21, 34.42, 29.86, 29.27, 29.03, 28.95, 26.74, 24.87, 14.18 (Figure S1). HRMS (ESI) *m/z* [M+H]<sup>+</sup> calcd for C<sub>21</sub>H<sub>31</sub>ClF<sub>3</sub>N<sub>2</sub>O<sub>3</sub>, 451.1970; found, 451.1973.

**Ethyl 12-[[3-chloro-5-(trifluoromethyl)phenyl]carbamoylamino]dodecanoate (6b).** White solid, 56 % yield. <sup>1</sup>H NMR (500 MHz, CDCl<sub>3</sub>): δ 7.71 (s, 1H), 7.63 (s, 1H), 7.44 (s, 1H), 7.18 (s, 1H), 5.48 (t, J=5.5 Hz, 1H), 4.13 (q, J=7.5 Hz, 2H), 3.22 (q, J=7.0 Hz, 2H), 2.30 (t, J=7.0 Hz, 2H), 1.60 (quin, J=7.0 Hz, 2H), 1.47 (quin, J=7.0 Hz, 2H), 1.35–1.20 (m, 17H). <sup>13</sup>C NMR (125 MHz, CDCl<sub>3</sub>): δ 174.81, 155.54, 141.28, 135.41, 132.56 (q, J=31 Hz), 126.56, 123.30 (q, J=272 Hz),

121.82, 119.16 (q,  $J=6$  Hz), 113.72 (q,  $J=6$  Hz), 60.60, 40.41, 34.58, 30.02, 29.45, 29.34, 29.30, 29.25, 29.20, 29.11, 26.91, 25.05, 14.34 (Figure S2). HRMS (ESI)  $m/z$   $[M+H]^+$  calcd for  $C_{22}H_{33}ClF_3N_2O_3$ , 465.2126; found, 465.2125.

**Ethyl 15-[[5-chloro-3-(trifluoromethyl)phenyl]carbamoylamino]pentadecanoate (6e).** White solid, 77% yield.  $^1H$  NMR (500 MHz,  $CDCl_3$ ):  $\delta$  7.66 (s, 1H), 7.62 (s, 1H), 7.43 (s, 1H), 7.18 (s, 1H), 5.48 (br, 1H), 4.13 (q,  $J=7.0$  Hz, 2H), 3.21 (q,  $J=7.0$  Hz, 2H), 2.31 (t,  $J=7.5$  Hz, 2H), 1.61 (quin,  $J=7.5$  Hz, 2H), 1.47 (quin,  $J=7.0$  Hz, 2H), 1.35–1.20 (m, 23H).  $^{13}C$  NMR (125 MHz,  $CDCl_3$ ):  $\delta$  174.75, 155.45, 141.22, 135.43, 132.57 (q,  $J=31$  Hz), 123.30 (q,  $J=272$  Hz), 121.88, 119.22 (q,  $J=6$  Hz), 113.77 (q,  $J=4$  Hz), 60.57, 40.49, 34.62, 30.09, 29.56, 29.52 (2 C), 29.42, 29.37, 29.27, 29.20, 26.98, 25.13, 14.35 (Figure S5). HRMS (ESI)  $m/z$   $[M+H]^+$  calcd for  $C_{25}H_{39}ClF_3N_2O_3$ , 507.2596; found, 507.2600.

### General Procedure for the Synthesis of Ureas from Nitriles

Nitriles **4a–b** (1.48 mmol) and  $NiCl_2 \cdot 6H_2O$  (0.704 g, 2.96 mmol) were dissolved in methanol (20 mL). The solution was cooled to 0 °C, and  $NaBH_4$  (0.280 g, 7.4 mmol) was added slowly over 30 min. The reaction was allowed to warm to room temperature and stirred for 1.5 h, then 1 M HCl was added until the resultant precipitate dissolved. The solution was made alkaline with  $NH_4OH$  and the reaction mixture was extracted with dichloromethane (3x50 mL). The organic layer was dried over  $Na_2SO_4$  and concentrated under reduced pressure. The residue was then dissolved in dichloromethane (15 mL), **5** (0.64 g, ~2.22 mmol) was added and the reaction mixture was stirred at room temperature for 2 h. The reaction mixture was then diluted with ethyl acetate (70 mL), washed with water (3x70 mL) and dried over  $Na_2SO_4$ . The extract was concentrated under reduced pressure, and the residue was purified on silica gel by stepwise gradient elution with dichloromethane/ethyl acetate (100:0–90:10), yielding the desired product as a white solid.

**Ethyl 13-[[5-chloro-3-(trifluoromethyl)phenyl]carbamoylamino]tridecanoate (6c).** White solid. Yield=82%.  $^1H$  NMR (500 MHz,  $CDCl_3$ ):  $\delta$  7.65 (s, 1H), 7.46 (s, 1H), 7.44 (s, 1H), 7.19 (s, 1H), 5.32 (t,  $J=5.5$  Hz, 1H), 4.13 (q,  $J=7.0$  Hz, 2H), 3.22 (q,  $J=6.5$  Hz, 2H), 2.31 (t,  $J=7.5$  Hz, 2H), 1.63 (quin,  $J=7.5$  Hz, 2H), 1.48 (quin,  $J=7.5$  Hz, 2H), 1.35–1.20 (m, 19H).  $^{13}C$  NMR (125 MHz,  $CDCl_3$ ):  $\delta$  174.82, 155.57, 141.27, 135.43, 132.54 (q,  $J=33$  Hz), 123.31 (q,  $J=272$  Hz), 119.16 (q,  $J=4$  Hz), 113.72 (q,  $J=4$  Hz), 60.60, 40.43, 34.60, 30.03, 29.46, 29.44, 29.41, 29.30, 29.29, 29.22, 29.15, 26.92, 14.34 (Figure S3). HRMS (ESI)  $m/z$   $[M+H]^+$  calcd for  $C_{23}H_{35}ClF_3N_2O_3$ , 479.2283; found, 479.2283.

**Ethyl 14-[[5-chloro-3-(trifluoromethyl)phenyl]carbamoylamino]tetradecanoate (6d).** White solid. Yield=74%.  $^1H$  NMR (500 MHz,  $CDCl_3$ ):  $\delta$  7.70 (s, 1H), 7.61 (s, 1H), 7.43 (s, 1H), 7.18 (s, 1H), 5.50 (br, 1H), 4.13 (q,  $J=7.0$  Hz, 2H), 3.22 (q,  $J=6.5$  Hz, 2H), 2.30 (t,  $J=7.5$  Hz, 2H), 1.61 (quin,  $J=7.5$  Hz, 2H), 1.47 (quin,  $J=7.5$  Hz, 2H), 1.35–1.20 (m, 21H).  $^{13}C$  NMR (125 MHz,  $CDCl_3$ ):  $\delta$  174.78, 155.57, 141.24,

135.41, 132.54 (q,  $J=33$  Hz), 123.30 (q,  $J=272$  Hz), 121.21, 119.17 (q,  $J=4$  Hz), 113.75 (q,  $J=4$  Hz), 60.58, 40.46, 34.61, 30.01, 29.56, 29.53, 29.51, 29.50, 29.40, 29.35, 29.29, 29.18, 26.96, 26.00, 14.34 (Figure S4). HRMS (ESI)  $m/z$   $[M+H]^+$  calcd for  $C_{24}H_{37}ClF_3N_2O_3$ , 493.2439; found, 493.2438.

### General Procedure for Ester Hydrolysis

**6a–e** (0.80 mmol) were dissolved in ethanol (30 mL) at 40 °C and 1.5 M sodium hydroxide (10 mL) was added dropwise and the reaction was stirred for 4 h. The reaction solvent was then decreased by half under reduced pressure, and then acidified with 1 M HCl to pH of 1–2. The resulting precipitate was then filtered, washed with water and then water/ethanol (1:1), and dried under reduced pressure.

**11-[[3-chloro-5-(trifluoromethyl)phenyl]carbamoylamino]undecanoic acid (7a).** White solid, mp=109–110 °C. Yield=85%.  $^1H$  NMR (500 MHz,  $d_6$ -DMSO):  $\delta$  9.02 (s, 1H), 7.76 (m, 2H), 7.28 (s, 1H), 6.42 (t,  $J=5.5$  Hz, 1H), 3.06 (q,  $J=6.5$  Hz, 2H), 2.17 (t,  $J=7.5$  Hz, 2H), 1.47 (quin,  $J=7.5$  Hz, 2H), 1.42 (quin,  $J=7.5$  Hz, 2H), 1.30–1.20 (m, 12H).  $^{13}C$  NMR (125 MHz,  $d_6$ -DMSO):  $\delta$  174.55, 154.72, 143.05, 134.06, 130.92 (q,  $J=32$  Hz), 123.38 (q,  $J=271$  Hz), 120.29, 116.68 (q,  $J=4$  Hz), 112.32 (q,  $J=4$  Hz), 33.71, 29.54, 28.96, 28.85, 28.73, 28.55, 26.34, 24.51 (Figure S6). HRMS calcd for  $C_{19}H_{27}ClF_3N_2O_3$  ( $[M+H]^+$ )  $m/z$ : 423.1653; found 423.1657.

**12-[[3-chloro-5-(trifluoromethyl)phenyl]carbamoylamino]dodecanoic acid (7b).** White solid, mp=110–111 °C. Yield=92%.  $^1H$  NMR (500 MHz,  $d_6$ -DMSO):  $\delta$  9.00 (s, 1H), 7.76 (m, 2H), 7.28 (s, 1H), 6.40 (t,  $J=5.5$  Hz, 1H), 3.07 (q,  $J=6.5$  Hz, 2H), 2.17 (t,  $J=7.5$  Hz, 2H), 1.48 (quin,  $J=7.5$  Hz, 2H), 1.42 (quin,  $J=7.5$  Hz, 2H), 1.30–1.20 (m, 14H).  $^{13}C$  NMR (125 MHz,  $d_6$ -DMSO):  $\delta$  174.46, 154.68, 143.00, 134.04, 130.96 (q,  $J=32$  Hz), 123.40 (q,  $J=271$  Hz), 120.27, 116.68 (q,  $J=4$  Hz), 112.30 (q,  $J=4$  Hz), 33.64, 29.54, 29.00, 28.93, 28.90, 28.74 (2 C), 28.54 (Figure S7). HRMS calcd for  $C_{20}H_{29}ClF_3N_2O_3$  ( $[M+H]^+$ )  $m/z$ : 437.1813; found 437.1815.

**13-[[3-chloro-5-(trifluoromethyl)phenyl]carbamoylamino]tridecanoic acid (7c).** White solid, mp=108–109 °C. Yield=90%.  $^1H$  NMR (500 MHz,  $d_6$ -DMSO):  $\delta$  9.27 (s, 1H), 7.77 (m, 2H), 7.25 (s, 1H), 6.63 (t,  $J=5.5$  Hz, 1H), 3.05 (q,  $J=6.5$  Hz, 2H), 2.15 (t,  $J=7.5$  Hz, 2H), 1.47 (quin,  $J=7.5$  Hz, 2H), 1.41 (quin,  $J=7.5$  Hz, 2H), 1.30–1.20 (m, 16H).  $^{13}C$  NMR (125 MHz,  $d_6$ -DMSO):  $\delta$  174.88, 154.83, 143.19, 134.03, 130.93 (q,  $J=32$  Hz), 123.38 (q,  $J=271$  Hz), 120.23, 116.54 (q,  $J=4$  Hz), 112.29 (q,  $J=4$  Hz), 34.08, 29.56, 29.01, 28.96, 28.95, 28.91, 28.75 (2 C), 28.61, 26.34, 24.67 (Figure S8). HRMS calcd for  $C_{21}H_{31}ClF_3N_2O_3$  ( $[M+H]^+$ )  $m/z$ : 451.1970; found 451.1972.

**14-[[3-chloro-5-(trifluoromethyl)phenyl]carbamoylamino]tetradecanoic acid (7d).** White solid, mp=112–114 °C. Yield=78%.  $^1H$  NMR (500 MHz,  $d_6$ -DMSO):  $\delta$  8.97 (s, 1H), 7.76 (m, 2H), 7.28 (s, 1H), 6.38 (t,  $J=5.5$  Hz, 1H), 3.07 (q,  $J=6.5$  Hz, 2H), 2.19 (t,  $J=7.5$  Hz, 2H), 1.47 (quin,  $J=7.5$  Hz, 2H), 1.42 (quin,  $J=7.5$  Hz, 2H), 1.30–1.20 (m, 18H).  $^{13}C$  NMR (125 MHz,  $d_6$ -DMSO):  $\delta$  174.46, 154.68,

143.00, 134.04, 130.96 (q,  $J=32$  Hz), 123.38 (q,  $J=271$  Hz), 120.27, 116.68 (q,  $J=4$  Hz), 112.32 (q,  $J=4$  Hz), 33.64, 29.52, 28.99 (2 C), 28.97, 28.90, 28.74, 28.72, 28.53, 26.29, 24.48 (Figure S9). HRMS calcd for  $C_{22}H_{37}ClF_3N_2O_3$  ( $[M+H]^+$ )  $m/z$ : 465.2126; found 465.2126.

**15-[[3-chloro-5-(trifluoromethyl)phenyl]carbamoylamino]pentadecanoic acid (7e).** White solid, mp=95–96°C. Yield=84%.  $^1H$  NMR (500 MHz,  $d_6$ -DMSO):  $\delta$  8.97 (s, 1H), 7.75 (m, 2H), 7.24 (s, 1H), 6.36 (t,  $J=5.5$  Hz, 1H), 3.07 (q,  $J=6.5$  Hz, 2H), 2.16 (t,  $J=7.5$  Hz, 2H), 1.47 (quin,  $J=7.5$  Hz, 2H), 1.42 (quin,  $J=7.5$  Hz, 2H), 1.30–1.20 (m, 20H).  $^{13}C$  NMR (125 MHz,  $d_6$ -DMSO):  $\delta$  174.48, 154.70, 143.05, 134.07, 130.95 (q,  $J=32$  Hz), 123.35 (q,  $J=271$  Hz), 120.26, 116.62 (q,  $J=4$  Hz), 112.33 (q,  $J=4$  Hz), 33.68, 29.59, 29.10 (2 C), 29.06 (2 C), 29.05, 28.98, 28.81, 28.79, 28.61 (Figure S10). HRMS calcd for  $C_{23}H_{35}F_3N_2O_3$  ( $[M+H]^+$ )  $m/z$ : 479.2283; found 479.2279.

**Biochemicals.** Low Glucose Dulbecco's Modified Eagle's Medium (DMEM-low glucose) and phosphate-buffered saline (PBS), dimethyl sulfoxide (DMSO), and bovine serum albumin were purchased from Sigma-Aldrich. Trypsin/EDTA, Fetal bovine serum (FBS), penicillin and streptomycin, 11-[2,2-difluoro-12-[(1*E*,3*E*)-4-phenylbuta-1,3-dienyl]-3-aza-1-azonia-2-boranuidatricyclo[7.3.0.0<sup>3,7</sup>]dodeca-1(12),4,6,8,10-pentaen-4-yl]undecanoic acid (C11 BODIPY™ 581/591; Lipid Peroxidation Sensor), Pierce™ BCA Protein Assay Kit, Hoechst 33342 stains, and Methanol were obtained from Thermo Fisher Scientific (Mulgrave, VIC, Australia). Sodium chloride, Tween 20, ethylenediaminetetraacetic acid (EDTA), and tris(hydroxymethyl)aminomethane were from Amresco LLC (Solon, OH). The annexin V-FITC/7-aminoactinomycin D (7-AAD) kit was purchased from Beckman Coulter (Lane Cove, NSW, Australia). The Cayman JC-1 (1,1',3,3'-tetraethyl-5,5',6,6'-tetrachloroimidacarbocyanine iodide) Mitochondrial Membrane Potential assay kit was from Sapphire Bioscience (Redfern, NSW, Australia). General analytical grade laboratory chemicals were obtained from LabScan (Lomb Scientific, Taren Point, NSW, Australia) or Ajax Chemicals (Sydney, NSW, Australia).

**Cell culture.** Human MDA-MB-231 breast cancer cells were purchased from ATCC (Manassas, VA, USA) and cultured in a 5% CO<sub>2</sub> humidified incubator at 37°C in DMEM-low glucose, supplemented with 10% FBS and 1% penicillin/streptomycin, essentially as described.<sup>[14]</sup> The cells were washed with PBS, harvested when 80–90% confluent using Trypsin/EDTA, and treated with different concentrations of **2** and **7a–e** in DMSO (final concentration 0.1%), while control cells were treated with DMSO alone. The well-differentiated non-tumorigenic MCF10 A control breast cell line was obtained from ATCC, and was maintained in DMEM-Nutrient Mixture F-12 containing cholera toxin, insulin, hydrocortisone, EGF, horse serum, and L-glutamine. Cell lines were free from mycoplasma.

**Annexin V-FITC/7-AAD assay.** MDA-MB-231 cells were seeded in 12-well plates ( $7 \times 10^4$  cells/well). Twenty-four h following serum removal, cells were treated with test compounds (10  $\mu$ M, 24 h), then harvested with trypsin-EDTA. Cells were harvested, washed with cold PBS, stained with annexin V-

FITC/7AAD, and analysed using a Gallios Flow Cytometer (Beckman Coulter, Lane Cove West, NSW, Australia).

**Clonogenic assay.** MDA-MB-231 cells were seeded in 6-well plates (300 cells/well) and then treated with test compounds (5  $\mu$ M) in serum-free medium. Twenty-four hours later, medium containing test compounds was replaced with fresh serum-containing medium, and plates were incubated for a further 12 days, with medium replacement at 3 day intervals. Cells were washed with cold PBS, fixed with methanol, stained with crystal violet and left to dry in air. Images from stained colonies were captured using a CKX41 inverted microscope (40x, magnification; Olympus Australia, Notting Hill, VIC) equipped with an Altra 20 camera (Olympus Australia) and colonies were quantified using Image J software (National Institutes of Health, Bethesda, MD).

**JC-1 plate assay.** MDA-MB-231 cells were seeded in 96-well plates ( $1 \times 10^4$  cells/well) and serum was removed after 24 h. Cells were treated with different concentrations of test compounds in DMSO (final concentration <0.1%) for 1 h, then incubated with JC-1 (1.5  $\mu$ M) in serum-free medium for 20 min (37°C). Following serum removal, cells were washed three times with PBS (300 g, 5 min). The fluorescence of JC-1 aggregates and monomers was measured at excitation/emission wavelengths of 535/595 nm and 485/535 nm, respectively, with a SpectraMax Gemini XPS microplate spectrofluorometer (San Jose, CA).

**JC-1 fluorescence microscopy.** MDA-MB-231 cells were seeded on coverslips in 12-well plates ( $7 \times 10^4$  cells/well). Twenty-four h following serum removal, the cells were treated with test compounds (5  $\mu$ M, 1 h), washed twice with serum-free medium and then treated with 1% JC-1 and 1% Hoechst 33258 (20 min, 37°C). The fluorescence of JC-1 monomers (green), JC-1 aggregates (red), and nuclear staining by Hoechst 33258 (blue) was imaged using an Olympus BX51 Fluorescence Microscope (Olympus Australia).

**C11 BODIPY (581/591) lipid peroxidation assay.** C11-BODIPY (581/591) and flow cytometry were used to detect reactive oxygen species (ROS) formation after treatment of cells with **2** and **7a–e**. MDA-MB-231 cells were seeded in 6-well plates ( $1.5 \times 10^5$  cells/well). Twenty-four h following serum removal, cells were treated with test compounds (10  $\mu$ M, 4 h), then stained with C11 BODIPY™ (581/591 dye; 1  $\mu$ M, 30 min). Cells were detached from plates using trypsin/EDTA, harvested and washed with PBS for analysis on a Gallios Flow Cytometer (Beckman Coulter, Lane Cove West, NSW, Australia).

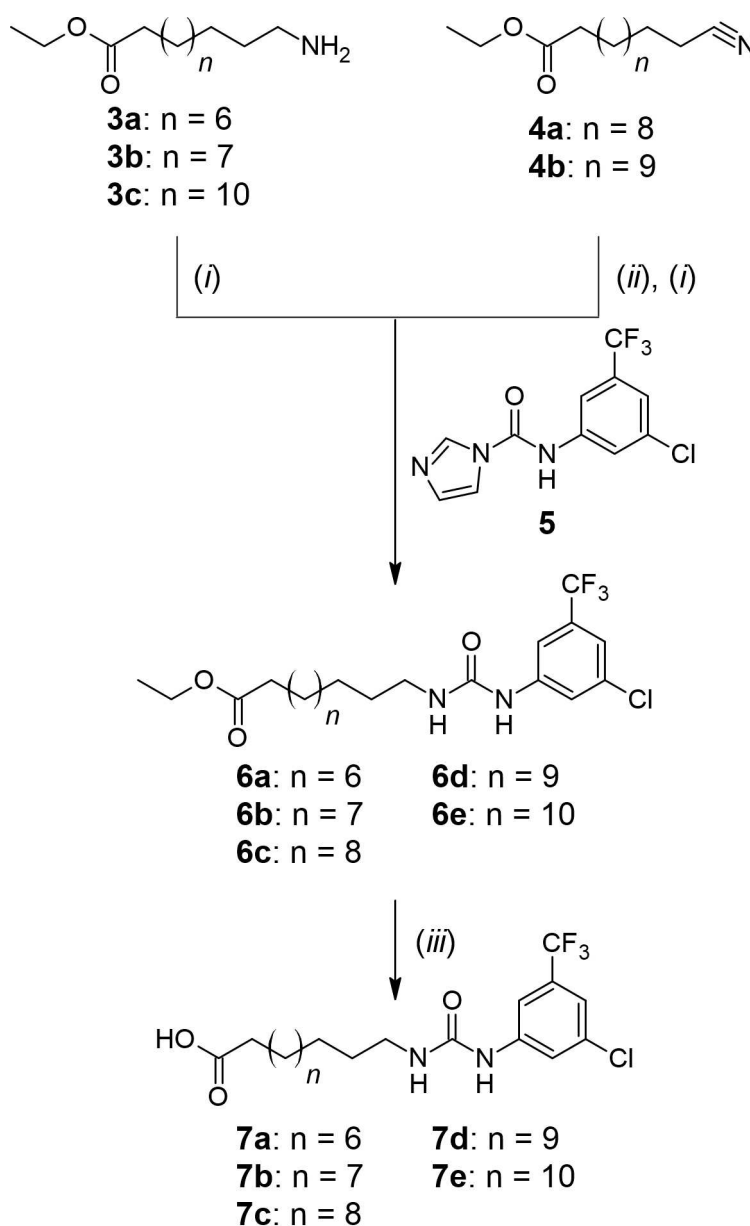
**Statistical analysis.** Data were derived from at least three independent experiments and are presented throughout as mean  $\pm$  SEM. Data were analysed by one-way ANOVA followed by Dunnett's multiple comparisons test (GraphPad Prism 5.0, GraphPad, San Diego, CA). Differences between two groups (control and treatment) were detected using the Student's *t*-test.

## Results

**Synthesis of aryl-urea fatty acid 2 and its chain contracted analogues.** The chain chain contracted analogues of 2 were synthesised as shown in Scheme 1. 7c (C13) and 7d (C14) were prepared from the nitriles 4a–b. In the first step the nitrile groups were reduced using sodium borohydride and nickel chloride. The crude amines were isolated by liquid-liquid extraction and immediately reacted with *N*-carbamoylimidazole 5, which was readily synthesised by reaction of 3-chloro-5-(trifluoromethyl)aniline with 1,1'-carbonyldiimidazole. In solution 5 dissociates to imidazole and 3-chloro-5-(trifluoromethyl)phenyl isocyanate; the isocyanate reacts with the amines to form the urea groups in 6c–d, and the reaction is catalysed by the liberated imidazole.<sup>[15]</sup> The remaining urea

intermediates 6a, 6b and 6c were similarly prepared from amines 3a–c by reaction with 5. In the final step the ester groups in 6a–e were hydrolysed with sodium hydroxide to afford the products 7a–e.

**Carbon chain length of aryl-urea fatty acids influences cell death in MDA-MB-231 cells.** The capacity of 2 and its chain-contracted analogues to promote MDA-MB-231 cell death was assessed using annexin V-FITC/7AAD staining. The induction of cell death varied with alkyl chain length. The proportion of cells exhibiting late apoptosis (dual staining, upper-right quadrant; Figure 2A) was significantly increased to  $5.3 \pm 1.3$ -fold ( $P < 0.0001$ ),  $3.4 \pm 0.7$ -fold ( $P < 0.05$ ) and  $4.8 \pm 0.9$ -fold ( $P < 0.001$ ) of control in cells after treatment with 7c, 7d, and 7e (10  $\mu$ M, 24 h), respectively (Figure 2B). In contrast, 2 failed to significantly increase the population of late-stage apoptotic cells



**Scheme 1.** Synthesis of 2 and the chain-contracted analogues 7a–e in which the alkyl chain length was varied. Reagents and conditions: (i) dichloromethane, 1 h; (ii)  $\text{NiCl}_2 \cdot 6\text{H}_2\text{O}$ ,  $\text{NaBH}_4$ ,  $0^\circ\text{C}$  – rt, 2 h; (iii) 1.5 M NaOH, ethanol/water, rt, 4 h.



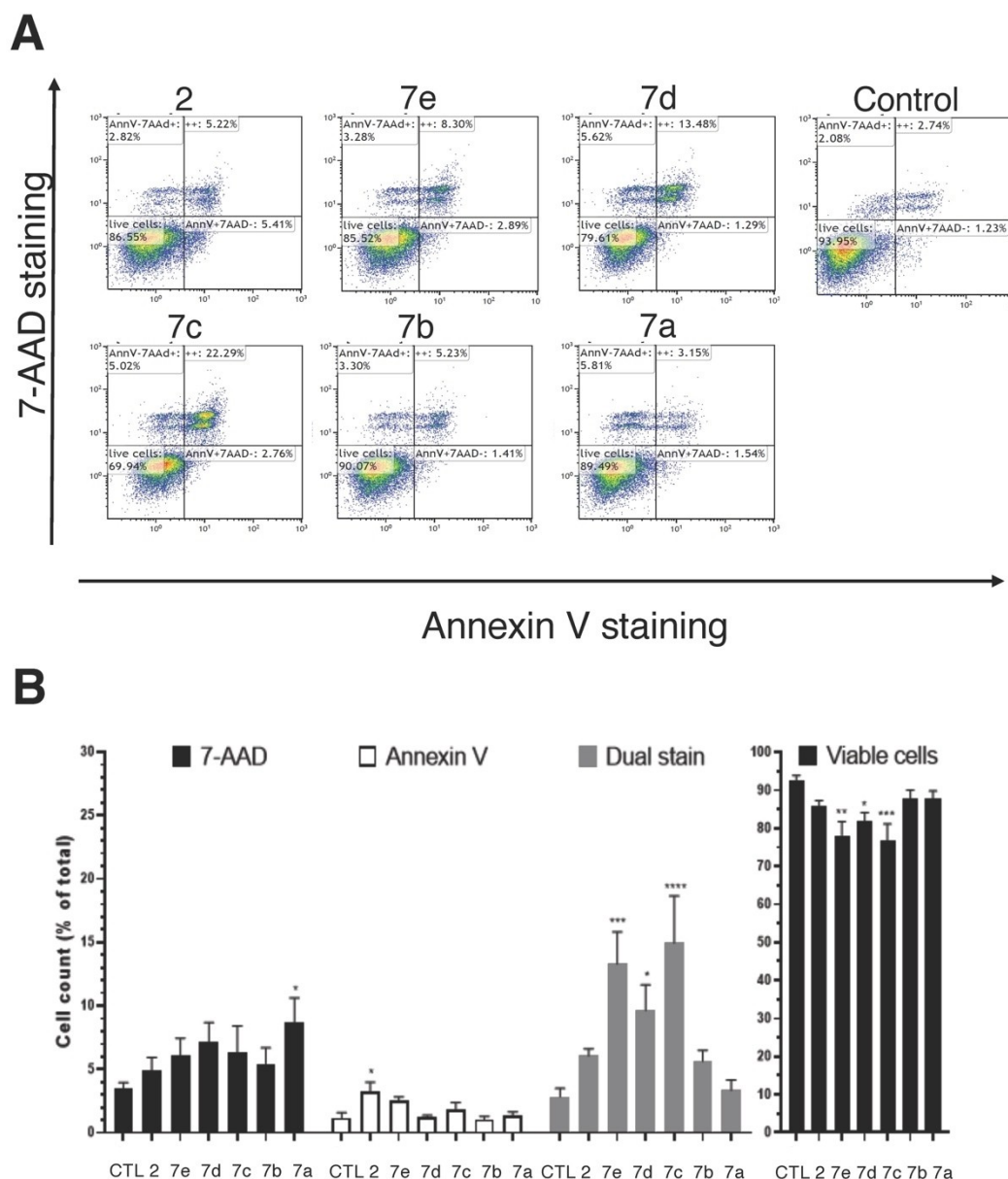


**Figure 2.** Annexin V-FITC/7-AAD staining in MDA-MB-231 cells treated with **2** and the chain-contracted analogues **7a–e** (10  $\mu$ M, 24 h). (A) representative images showing unstained viable cells (lower-left quadrant), annexin V-stained cells (lower-right quadrant), dual annexin V and 7-AAD-stained cells (upper-right quadrant), and 7-AAD-stained cells (upper-left quadrant). (B) Percentage of cells stained with annexin V, 7-AAD or both, and unstained viable cells. Data from at least three independent experiments were analysed via ANOVA followed by Dunnett's multiple comparisons test and are presented as mean  $\pm$  SEM. Different from DMSO-treated control: \* $P < 0.05$ , \*\* $P < 0.01$ , \*\*\* $P < 0.001$ , \*\*\*\* $P < 0.0001$ .

under these conditions. There was also an increase in early apoptosis (annexin V staining alone, lower-right quadrant;  $P < 0.05$ ; Figure 2B) after treatment with **2**, while **7a** increased the percentage of cells stained with 7-AAD alone (upper-left quadrant), consistent with DNA staining after disruption of the cell membrane ( $P < 0.05$ ; Figure 2B). The proportion of unstained viable cells (lower-left quadrant) significantly decreased after treatment with **7c–7e**, but not **2**. Total cell killing was calculated as the sum of annexin V-, 7-AAD- and dual-stained cells and was related to carbon chain length. Thus, **7c**, **7d** and **7d** increased total cell death to  $22.7 \pm 4.2\%$  ( $P < 0.01$ ),  $17.7 \pm 2.3$

( $P < 0.05$ ) and  $21.5 \pm 3.7\%$  ( $P < 0.01$ ) of total compared with control ( $7.2 \pm 1.4\%$ ; Figure S11).

A clonogenic assay was used to further assess the survival and recovery of MDA-MB-231 cells after treatment with selected **2** analogues.<sup>[16]</sup> The number of colonies after 12 days decreased from  $60.7 \pm 10.5$  in DMSO control to  $2.33 \pm 1.2$  (\*\*\*\* $P < 0.0001$ ),  $2.67 \pm 0.67$  (\*\*\* $P < 0.001$ ),  $2.67 \pm 0.33$  (\*\*\* $P < 0.001$ ), and  $23.3 \pm 6.74$  (\*\* $P < 0.01$ ) with **2**, **7e**, **7c** and **7a**, respectively (Figure 3). The superior activity against oncogenic growth of **2**, **7e** and **7c** over the shortest analogue **7a** indicates that alkyl chain length determines the extent of cell survival after treatment (Figure 3).

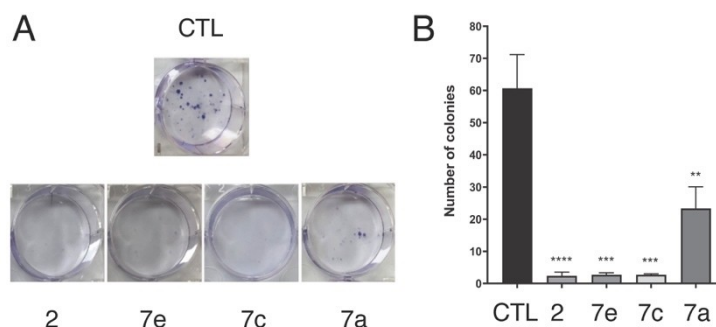


**Figure 3.** Effect of 2, 7e, 7c and 7a (5  $\mu$ M, 24 h) on the colony formation capacity of MDA-MB-231 cells. (A) representative images of crystal violet stained colony growth after 12 days. (B) Quantification of colony formation. Data are mean  $\pm$  SEM of three independent experiments; one-way ANOVA + Dunnett's multiple comparisons test. \*\* $P < 0.01$ , \*\*\* $P < 0.001$ , \*\*\*\* $P < 0.0001$  relative to DMSO control.

**Chain contracted 2 analogues target the mitochondrion in MDA-MB-231 cells.** The lipophilic cationic dye JC-1 was used to detect mitochondrial involvement in the mechanism of action of 2 analogues. In viable cells with intact mitochondrial membrane and a high  $\Delta\Psi_m$ , JC-1 dye forms aggregates that fluoresce red.<sup>[17]</sup> However, when the mitochondrial membrane is disrupted and  $\Delta\Psi_m$  is low, JC-1 remains in the monomeric state and fluoresces green. Following treatment,  $IC_{50}$  concentrations were determined for 2 and its analogues (Table 1). The ranked order of compound activity in JC-1 assays reflected that observed in cell killing assays. Thus, 7c (C13) and 7d (C14) depolarised MDA-MB-231 cell mitochondria with  $IC_{50}$  concentrations of  $\sim 4 \mu$ M, while analogues with shorter or longer alkyl chains were less potent.

Because the  $IC_{50}$ s of the most potent analogues 7c, 7d and 2 were in the range  $\sim 5$ – $6 \mu$ M, the 5  $\mu$ M concentration was selected for further studies with JC-1. Using fluorescence microscopy, the agents, and especially 7c and 7d, increased the green fluorescence intensity (monomeric JC-1) and decreased the red fluorescence intensity (JC-1 aggregates; Fig-

ure 4). These findings indicate that 2 analogues disrupt the mitochondrial membrane potential and decrease the formation of red JC-1 aggregates in MDA-MB-231 cells.

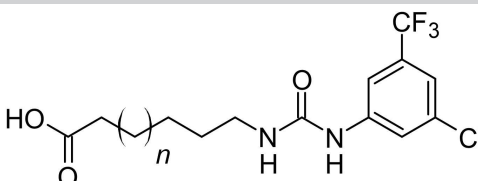
**Increased ROS production by 2 analogues in breast cancer cells.** Findings with JC-1 indicated that 2 and its analogues target the mitochondrion in MDA-MB-231 cells. Mitochondria are a major source of ROS production. In further studies, ROS generation was evaluated in MDA-MB-231 cells after 2 and 7a–e treatment using the fluorescent dye C11 BODIPY (581/591). C11 BODIPY (581/591) contains a polyunsaturated butadienyl moiety that is susceptible to peroxidation. Lipid peroxides shift the excitation and emission wavelengths from 581–500 nm and from 591–510 nm, respectively.<sup>[18]</sup> The C11 BODIPY (581/591) ratio was markedly increased after treatment for 4 h with 10  $\mu$ M 7c to  $1.271 \pm 0.245$  ( $P < 0.0001$ ) and, to a lesser extent, 2, 7e, 7d, 7b and 7a to  $0.661 \pm 0.073$  ( $P < 0.05$ ),  $0.776 \pm 0.064$  ( $P < 0.05$ ),  $0.789 \pm 0.042$  ( $P < 0.01$ ),  $0.782 \pm 0.052$  ( $P < 0.01$ ), and  $0.712 \pm 0.060$  ( $P < 0.05$ ), respectively, relative to control ( $0.278 \pm 0.029$ ; Figure 5A). These findings indicate that mitochondrial targeting with 2 and 7a–e promotes ROS production in MDA-MB-231 cells, and that 7c is the most effective agent in the series at promoting ROS production.

**Carbon chain length in 2 analogues controls mitochondrial targeting and cell killing.** Pearson's correlation analysis was undertaken to evaluate relationships between the disruption of  $\Delta\Psi_m$ , ROS generation and MDA-MB-231 cell killing. Cell death was correlated positively with increased ROS production ( $r = 0.79$ ,  $P < 0.05$ ; Figure 5B), while the JC-1 red:green fluorescence ratio was correlated negatively with cell death ( $r = -0.83$ ,  $P < 0.05$ ; Figure 5C; Table S1). These findings indicate that mitochondrial disruption and ROS production are greater with analogues that kill cells more efficiently. In support of these findings, ROS generation (C11 BODIPY (581/591) ratio) was well correlated with the JC-1 fluorescence ratio ( $r = -0.8453$ ,  $P$  value = 0.0166; Figure S12; Table S1).

## Discussion

Well-tolerated agents with novel mechanisms of anticancer action are required for the treatment of advanced breast cancer

**Table 1.**  $IC_{50}$ s for the disruption of the mitochondrial membrane potential in MDA-MB-231 cells by aryl-ureas.

<div style="text-align: center;">  <p><b>7a-e</b></p> </div>			
Aryl-urea ( $\mu$ M)	<i>n</i>	$IC_{50}$	$r^2$
2	11	$6.1 \pm 3.8$	0.92
7a	6	$10.5 \pm 2.3$	0.95
7b	7	$9.4 \pm 1.0$	0.95
7c	8	$4.8 \pm 0.8$	0.93
7d	9	$4.9 \pm 0.9$	0.97
7e	10	$9.0 \pm 1.4$	0.97

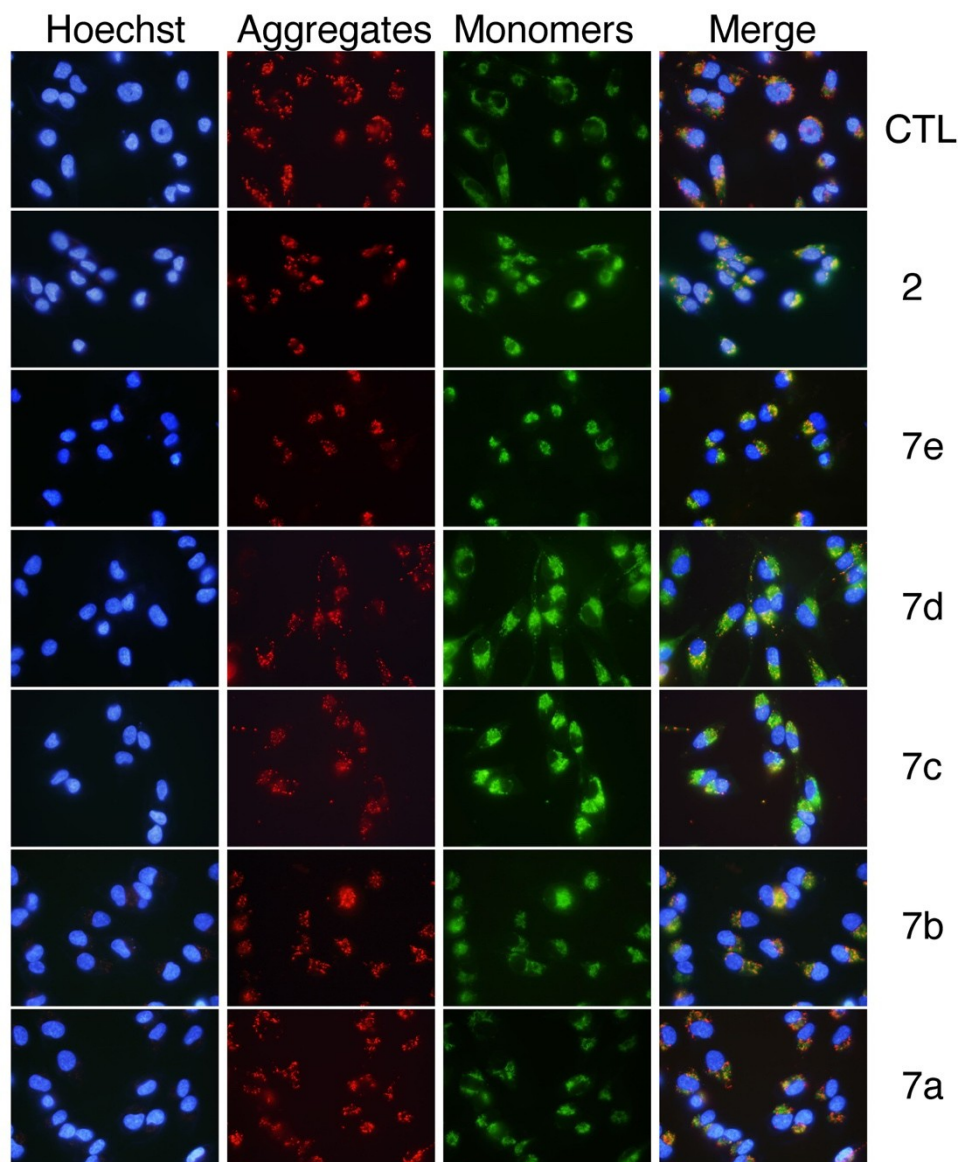


**Figure 4.** Fluorescence microscopy images of MDA-MB-231 cells showing the effect of **2** and the chain-contracted analogues **7a–e** (5  $\mu$ M, 1 h) on  $\Delta\Psi_m$ . Cells were incubated for 20 min with JC-1 and Hoechst dyes. Fluorescence images of JC-1 monomers (green), J-aggregates (red), and nucleus staining (blue) were captured using an Olympus BX51 fluorescence microscope. Representative images are shown.

and may offer the opportunity for further remissions in patients. In previous studies we demonstrated the capacity of epoxides derived from  $\omega$ -3 PUFAs and other  $\omega$ -3 epoxy-fatty acids to decrease cell viability.<sup>[6–8]</sup> CTU (**1**) is a metabolically stable aryl-urea mimic of these  $\omega$ -3 epoxy-fatty acids that selectively disrupts the mitochondrial membrane in cancer cells and generates ROS, which promotes cancer cell death.<sup>[12,19]</sup> However, the relatively low potency of **1** highlights the need for structural optimisation to enable the identification of potential lead compounds for drug development. In a recent study, we found that **2** had improved activity over the prototype agent **1**.<sup>[13]</sup> The present study sought to further evaluate the potential of **2** in greater detail using a new series of chain-contracted analogues. The principal finding to emerge was that the analogue **7c**, in which the carbon chain was three methylene units shorter than

in **2**, had superior anticancer activity due to enhanced mitochondrial targeting capacity.

In cancer cells the structure and function of the mitochondrion is modified, which enables adaptation to the increased requirements for cellular replication.<sup>[2]</sup> In this study, mitochondrial disruption was reflected by measurement of the JC-1 red: green fluorescence ratio. **7c** was the most active of the congeners ( $IC_{50}$   $4.8 \pm 0.8$   $\mu$ M), followed by the longer chain agents, while the short chain analogues were the least effective. Consistent with JC-1 findings, intermediate chain analogues, especially **7c**, increased cell death most effectively. The annexin V/7AAD staining ratio was used to quantify the relative importance of apoptosis and necrosis. Annexin V detects phosphatidylserine residues in the plasma membrane that are externalized during apoptosis, while disruption of the plasma



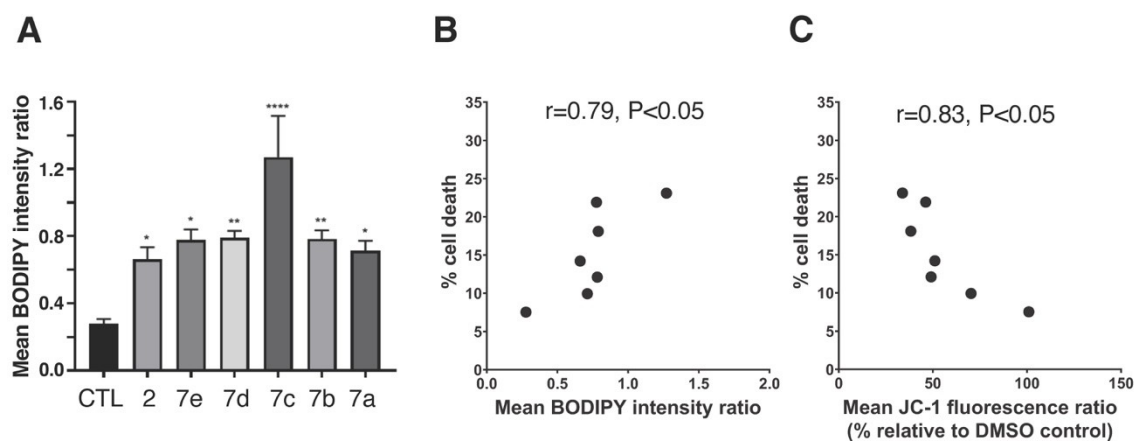


**Figure 5.** (A) ROS generation, as reflected by the C11 BODIPY (581/591) intensity ratio, in MDA-MB-231 cells after treatment with **2** and the chain-contracted analogues **7a–e** (10  $\mu$ M, 4 h). (B,C) Pearson's correlation analysis of data with the analogues showing (B) the relationship between increased ROS production (C11 BODIPY (581/591) intensity ratio) and cell death (the sum of annexin-, 7-AAD and dual-stained cells), and (C) the relationship between mitochondrial membrane potential (after JC-1 staining) and cell death. Data are mean  $\pm$  SEM of at least three independent experiments; ANOVA + Dunnett's multiple comparisons test. Different from DMSO-treated control: \* $P < 0.05$ , \*\* $P < 0.01$ , \*\*\*\* $P < 0.0001$ .

membrane activates necrosis and enables DNA staining by 7AAD. An increase in early apoptosis was produced by **7a** while necrosis was increased somewhat by **2**. Overall **7a** and **2** produced staining ratios that were not significantly different from control, suggesting that both cell death pathways were increased similarly. Total cell death was estimated as the sum of annexin V-, 7-AAD and dual-stained cells and indicated that **7c**, **7e** and **7d** were highly effective in cell killing. Data from clonogenic assays were consistent with findings from annexin V/7AAD staining.

Some information has been reported on the structural requirements for anticancer activity of  $\omega$ -3 PUFA epoxide-derived aryl-ureas. Simple alkyl urea analogues of epoxy-fatty acids were poorly active.<sup>[7]</sup> However, inclusion of a substituted terminal aryl system in the simple ureas led to the identification of the aryl-urea **1** as an active agent (Figure 1). **1** targeted the cancer cell mitochondrion, activated cell killing and decreased ATP production *in vitro*.<sup>[12]</sup> Active aryl-ureas all contained lipophilic, strongly electron-withdrawing groups in the meta- and para-positions of the terminal aromatic system.<sup>[13]</sup>

Other structural modifications have also produced promising analogues. Bioisosteric replacement of the **1** terminal carboxylate with sulfonic acid and oxo-thiadiazole produced active analogues.<sup>[20]</sup> The corresponding hydroxamic acid analogue was also active, although the onset of cell killing was slower.<sup>[20]</sup> More recently, a different bioisosteric strategy was tested in which an in-chain methylene group in **1** was replaced by a sulfur atom to produce 3-thia-**1**. This agent showed a several-fold greater capacity than **1** to elicit mitochondrial disruption and cancer cell killing *in vitro*.<sup>[21]</sup> The present findings that **7c** was several-fold more active than **2** provides an additional approach to enhance the drug likeness of aryl-ureas. The loss of three methylene units corresponds to an approximate decrease in clog P of 1.5, reflecting decreased hydrophobic character.<sup>[22]</sup> It would now be of interest to incorporate

combinations of these bioisosteric replacements that improved the activity of **1** in a drug development program based on **7c**.

## Conclusions

The cancer cell mitochondrion is a promising anticancer drug target because it controls cell death and energy production and is structurally and functionally different from normal cell mitochondria.<sup>[1,2]</sup> We have shown previously that the aryl-urea **1** uncoupled the electron transport chain after mitochondrial entry leading to impaired ATP formation and increased ROS production.<sup>[24]</sup> If ROS exceed a certain critical limit, the antioxidant defence is overwhelmed, which leads to oxidative damage to DNA, lipids, and proteins, and activates apoptosis and/or necrosis.<sup>[19]</sup> The production of ROS was required in cell death and followed the activation of endoplasmic reticulum stress.<sup>[23]</sup> In the present study, **2** analogues, especially **7c**, strongly increased ROS production and activated cancer cell death to a greater extent than **1**. In conclusion, the enhanced activity and improved drug-like properties of **7c** suggests that it may be a suitable lead molecule for a drug development program of aryl-ureas as anticancer agents.

## Abbreviations

7-AAD	7-aminoactinomycin D
C11	BODIPY (581/591, 11-[2,2-difluoro-12-[(1E,3E)-4-phenylbuta-1,3-dienyl]-3-aza-1-azonia-2-boranuidatricyclo[7.3.0.0.3,7]dodeca-1(12),4,6,8,10-pentaen-4-yl]undecanoic acid
CTU	16-([4-chloro-3-(trifluoromethyl)phenyl]carbamoylamino)hexadecanoic acid
CYP	cytochrome P450

DMEM	Dulbecco's Modified Eagle's Medium
DMSO	dimethylsulfoxide
EPA	eicosapentaenoic acid
FBS	fetal bovine serum
HRMS	High Resolution Mass Spectrometry
JC-1	1,1',3,3'-tetraethyl-5,5',6,6'-tetrachloroimidacarbocyanine iodide
PBS	phosphate-buffered saline
$\omega$ -3 PUFA	$\omega$ -3 polyunsaturated fatty acid
ROS	reactive oxygen species

## Author Contributions

Conceptualization: MM, TR; Data curation: YE, TR, MM; Formal Analysis: YE, AR, MKR, TR, MM; Funding acquisition: MM; Investigation: YE, AR, MKR; Methodology: MKR, TR; Project administration: MM; Resources: YE, AR, MKR, TR, MM; Supervision: MM, TR; Writing – original draft: YE; Writing – review & editing: YE, AR, MKR, TR, MM.

## Acknowledgements

This study was supported by grants from the Australian National Health and Medical Research Council (1031686 and 1145424). Open Access publishing facilitated by The University of Sydney, as part of the Wiley - The University of Sydney agreement via the Council of Australian University Librarians.

## Conflict of Interests

The authors declare no conflict of interest.

## Data Availability Statement

The data that support the findings of this study are available from the corresponding author upon reasonable request.

**Keywords:** Antitumor agents · Apoptosis · Breast cancer · Lipid drugs · Mitochondrion

- [1] C. Wang, R. J. Youle, *Annu. Rev. Genet.* **2009**, *43*, 95–118.
- [2] S. Fulda, L. Galluzzi, G. Kroemer, *Nat. Rev. Drug Discov.* **2010**, *9*, 447–464.
- [3] D. P. Rose, J. M. Connolly, *J. Natl. Cancer Inst.* **1993**, *85*, 1743–1747.
- [4] W. E. Hardman, *J. Nutr.* **2002**, *132*, 3508 s–3512 s.
- [5] M. Murray, A. Hraiki, M. Bebawy, C. Pazderka, T. Rawling, *Pharmacol. Ther.* **2015**, *150*, 109–128.
- [6] P. H. Cui, N. Petrovic, M. Murray, *Br. J. Pharmacol.* **2011**, *162*, 1143–1155.
- [7] H. R. E. Dyari, T. Rawling, K. Bourget, M. Murray, *J. Med. Chem.* **2014**, *57*, 7459–7464.
- [8] H. R. E. Dyari, T. Rawling, Y. Chen, W. Sudarmana, K. Bourget, J. M. Dwyer, S. E. Allison, M. Murray, *FASEB J.* **2017**, *31*, 5246–5257.
- [9] G. Zhang, D. Panigrahy, L. M. Mahakian, J. Yang, J. Y. Liu, K. S. Stephen Lee, H. I. Wettersten, A. Ulu, X. Hu, S. Tam, S. H. Hwang, E. S. Ingham, M. W. Kieran, R. H. Weiss, K. W. Ferrera, B. D. Hammock, *Proc. Natl. Acad. Sci. U. S. A.* **2013**, *110*, 6530–6535.
- [10] J. R. Falck, R. Kodala, R. Manne, K. R. Atcha, N. Puli, N. Dubasi, V. L. Manthathi, J. H. Capdevila, X. Y. Yi, D. H. Goldman, C. Morisseau, B. D. Hammock, W. B. Campbell, *J. Med. Chem.* **2009**, *52*, 5069–5075.
- [11] J. R. Falck, G. Wallukat, N. Puli, M. Goli, C. Arnold, A. Konkel, M. Rothe, R. Fischer, D. N. Müller, W. H. Schunk, *J. Med. Chem.* **2011**, *54*, 4109–4118.
- [12] T. Rawling, H. Choucair, N. Koolaji, K. Bourget, S. E. Allison, Y. J. Chen, C. R. Dunstan, M. Murray, *J. Med. Chem.* **2017**, *60*, 8661–8666.
- [13] Y. Al-Zubaidi, C. W. Pazderka, N. Koolaji, M. K. Rahman, H. Choucair, B. Umashankar, K. Bourget, Y. Chen, T. Rawling, M. Murray, *Eur. J. Pharm. Sci.* **2019**, *129*, 87–98.
- [14] P. H. Cui, T. Rawling, K. Bourget, T. Kim, C. C. Duke, M. R. Doddareddy, D. E. Hibbs, F. Zhou, B. N. Tattam, N. Petrovic, M. Murray, *J. Med. Chem.* **2012**, *55*, 7163–7172.
- [15] T. Rawling, A. M. McDonagh, B. Tattam, M. Murray, *Tetrahedron* **2012**, *68*, 6065–6070.
- [16] N. A. Franken, H. M. Rodermond, J. Stap, J. Haveman, C. Van Bree, *Nat. Protoc.* **2006**, *1*, 2315–2319.
- [17] M. Reers, T. W. Smith, L. B. Chen, *Biochemistry* **1991**, *30*, 4480–4486.
- [18] G. P. Drummen, L. C. van Liebergen, J. A. Op den Kamp, J. A. Post, *Free Radic. Biol. Med.* **2002**, *33*, 473–490.
- [19] M. Schieber, N. S. Chandel, *Curr. Biol.* **2014**, *24*, R453–R462.
- [20] N. Koolaji, T. Rawling, K. Bourget, M. Murray, *ChemMedChem* **2018**, *13*, 1036–1043.
- [21] M. K. Rahman, B. Umashankar, H. Choucair, C. Pazderka, K. Bourget, Y. Chen, C. R. Dunstan, T. Rawling, M. Murray, *Eur. J. Pharmacol.* **2023**, *939*, 175470.
- [22] C. Hansch, A. Leo, S. H. Unger, K. H. Kim, D. Nikaitani, E. J. Lien, *J. Med. Chem.* **1973**, *16*, 1207–1216.
- [23] H. Choucair, M. K. Rahman, B. Umashankar, Y. Al-Zubaidi, K. Bourget, Y. Chen, C. Dunstan, T. Rawling, M. Murray, *Cancer Lett.* **2022**, *526*, 131–141.
- [24] T. Rawling, H. MacDermott-Opeskin, A. Roseblade, C. Pazderka, C. Clarke, K. Bourget, X. Wu, W. Lewis, B. Noble, P. A. Gale, M. L. O'Mara, C. Cranfield, M. Murray, *Chem. Sci.* **2020**, *11*, 12677–12685.

Manuscript received: April 19, 2024  
Revised manuscript received: June 23, 2024  
Accepted manuscript online: June 30, 2024  
Version of record online: August 19, 2024